Front. Earth Sci. 2023, 17(2): 361−377
https://doi.org/10.1007/s11707-022-0995-0

RESEARCH ARTICLE

Runoff components and the contributions of precipitation and temperature in a highly glacierized river basin in Central Asia

Anqian WANG[1], Buda SU (✉)[2,3], Jinlong HUANG[2], Cheng JING[3], Zbigniew W. KUNDZEWICZ[2,4], Hui TAO[3], Mingjin ZHAN[5], Tong JIANG[2]

1 College of Geography and Environment, Shandong Normal University, Jinan 250358, China
2 Collaborative Innovation Center on Forecast and Evaluation of Meteorological Disaster/Institute for Disaster Risk Management/ School of Geography Science, Nanjing University of Information Science & Technology, Nanjing 210044, China
3 State Key Laboratory of Desert and Oasis Ecology, Xinjiang Institute of Ecology and Geography, Chinese Academy of Sciences, Urumqi 830011, China
4 Institute for Agricultural and Forest Environment, Polish Academy of Sciences, Poznan 60809, Poland
5 Jiangxi Eco-meteorological Center, Nanchang 330000, China

Abstract Understanding the main drivers of runoff components and contributions of precipitation and temperature have important implications for water-limited inland basins, where snow and glacier melt provide essential inputs to surface runoff. To quantify the impact of temperature and precipitation changes on river runoff in the Tarim River basin (TRB), the Hydrologiska Byrans Vattenbalansavdelning (HBV)-light model, which contains a glacier routine process, was applied to analyze the change in runoff composition. Runoff in the headstream parts of the TRB was more sensitive to temperature than to precipitation. In the TRB, overall, rainfall generated 41.22% of the total runoff, while snow and glacier meltwater generated 20.72% and 38.06%, respectively. These values indicate that temperature exerted more major effects on runoff than did precipitation. Runoff compositions were different in the various subbasins and may have been caused by different glacier coverages. The runoff volumes generated by rainfall, snowmelt, glacier melt was almost equal in the Aksu River subbasin. In the Yarkand and Hotan River subbasins, glacier meltwater was the main supplier of runoff, accounting for 46.72% and 58.73%, respectively. In the Kaidu-Kongque River subbasin, 80.86% was fed by rainfall and 19.14% was fed by snowmelt. In the TRB, runoff generated by rainfall was the dominant component in spring, autumn, winter, while glacier melt runoff was the dominant component in summer. Runoff in the TRB significantly increased during 1961–2016; additionally, 56.49% of the increase in runoff was contributed by temperature changes, and 43.51% was contributed by precipitation changes. In spring, the runoff increase in the TRB was mainly caused by the precipitation increase, opposite result in summer and autumn. Contribution of temperature was negative in winter. Our findings have important implications for water resource management in high mountainous regions and for similar river basins in which melting glaciers strongly impact the hydrological cycle.

Keywords runoff components, glacier meltwater, contribution, HBV-light model, Tarim River basin

1 Introduction

Glacierized basins in high mountainous regions are representative of the head watersheds of downstream rivers and provide abundant water resources for ecological environments, agricultural irrigation, and drinking water supplies in the lower reaches (Immerzeel et al., 2013; Pritchard, 2019; Nie et al., 2021). The runoff in these basins mainly consists of rainfall, snowmelt, and glacier melt (Lutz et al., 2014). Air temperature and precipitation have strong seasonality and play a key role in regulating the seasonal flow advantage of a specific water source. Runoff from glacierized basins is highly vulnerable to current climate change. Increasing temperatures could accelerate glacier melt and snowmelt in these river basins (Xu. et al., 2017; Huang et al., 2018; Wang et al., 2018, 2019a; He et al., 2021), resulting in increased meltwater supplies to rivers in the near-term. Quantifying

Received October 31, 2021; accepted April 7, 2022

E-mail: subd@nuist.edu.cn

* Anqian WANG and Buda SU contributed equally to this work.

the contributions of different runoff components to river runoff is critical for understanding the dynamics of water resource availability in these basins.

The Tarim River basin is one of the world's largest endorheic river basins and is dominated by an arid inland climate (Chen et al., 2007, 2009; Tao et al., 2011; Su et al., 2016, 2017; Huang et al., 2018; Wang et al., 2020, 2021; Bolch et al., 2022). Precipitation in the Tarim River basin has shown an increasing trend (Shi et al., 2003; Tao et al., 2011; Li et al., 2020; Bolch et al., 2022), while the snow area coverage has decreased over the last few decades (Farinotti et al., 2015; Chen et al., 2019). The Tarim River basin can be divided into five major parts: the Aksu River subbasin, Yarkand River subbasin, Hotan River subbasin, Kaidu-Kongque River subbasin, and mainstream area, which are also referred to as the "four source streams and one mainstream" (Ye et al., 2014a, 2014b). Among the four source streams, only three headwaters, including the Aksu, Yarkand, and Hotan Rivers, have a surface water connection relationship with the mainstream (Xu et al., 2010; Ye et al., 2014a, 2014b; Wang et al., 2021). These three rivers are associated with the upstream Tarim River basin, while the Kaidu-Kongque River transports water to the lower reaches from Bostan Lake to the downstream Tarim River mainstream through the Kuta Main Canal (Chen et al., 2009; Xu et al., 2010; Zhang et al., 2014) (more details are shown in Fig. 1). Studies have shown that runoff from the Tarim River basin has been increasing, while the runoff changes from the "four sources" of these basins are different (Chen et al., 2009; Huang et al., 2018). The changes in runoff from the Aksu, Yarkand, and Kaidu-Kongque Rivers are significantly increasing, and the changes in runoff from the Hotan River are non-significantly increasing (Zhang and Zuo, 2017).

Studies on runoff composition have focused mainly on the Aksu River, which is the most important tributary of the Tarim River (Duethmann et al., 2015; Bolch et al., 2022), but the conclusions of these studies were not consistent due to their different hydrological models and methods. For example, the variable infiltration capacity (VIC) hydrological model integrated with an energy-balanced ice-melt module was applied to the Kumarik River, which is the left branch of the Aksu River, and the results revealed that glacier melt, snowmelt, and rainfall runoff accounted for 43.8%, 27.7%, and 28.5% of the runoff composition, respectively (Zhao et al., 2013). Similarly, a study using the Water Availability in Semi-Arid environments (WASA) hydrological model, which contains a glacier mass balance module, showed that the contribution from glacier melt to river runoff was approximately 35%–48% (Duethmann et al., 2015), while the contribution was 30%–48% when the soil and water assessment tool (SWAT) hydrological model, which contains a degree-day glacier melt algorithm, was applied (Ji et al., 2019). A higher contribution of 59% from glacier meltwater was detected during the glacier melt period (July–August) by isotope-based end-member mixing analysis (Chen et al., 2019). For the right branch of the Aksu River, namely, the Toshkan River, the contribution of glacier melt to river runoff was estimated to be 23.0% and 9%–24% by Zhao et al. (2013) and Duethmann et al. (2015), respectively, and this value was estimated to be 39% in July–August by Chen et al. (2019). Although valuable findings have been achieved in the Aksu River basin, a lack of information from other subbasins might lead to an inadequate understanding of climate change impacts on the river regime in the Tarim River basin.

Because of climate change, runoff from the headwaters

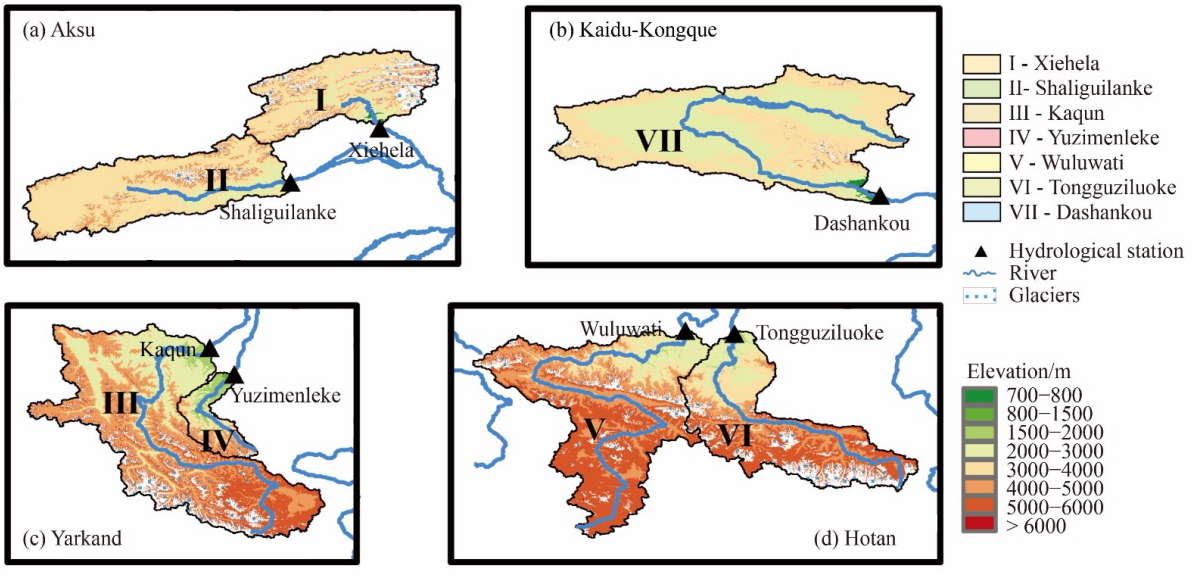

Fig. 1 Location of the four source regions and main hydrological stations in the Tarim River basin; (a) Aksu River subbasin; (b) Kaidu-Kongque River subbasin; (c) Yarkand River subbasin; (d) Hotan River subbasin.

of the Tarim River basin has undergone obvious changes that have significantly affected downstream areas. It is necessary to quantitatively evaluate the impact of climate change on runoff. Temperature and precipitation are the main factors driving streamflow changes (Duethmann et al., 2015; Chen et al., 2019; Wu et al., 2020; Xin et al., 2021). Li and Fang (2021) adopted the SWAT hydrological model to assess climate change impacts on the streamflow of the Mun River in the Mekong Basin and found that temperature played a more important role during the dry season, while precipitation was more significant during the wet season. Wang et al. (2021) revealed the dominant climate factors affecting runoff changes in all three naturally connected tributaries in the Tarim River basin by combining the glacier-enhanced SWAT model with the original and detrended precipitation and temperature inputs. It was recognized that rising temperatures contributed 94% and 66% to the streamflow increases in the Hotan and Aksu River subbasins, respectively, and precipitation contributed 87% to the runoff increases in the Yarkand River subbasin.

The main objective of this study was to analyze the effects of precipitation and temperature changes in recent decades on glacier melt, snowmelt, and streamflow in the glacier-dominated headwaters of the Tarim River basin. Quantitative conclusions drawn from this study may deepen the current understanding of the hydrological response of highly glacierized river basins to climate change. This study will lay the basis not only for future hydrological studies in the Tarim River basin but also for other similar river basins worldwide. To achieve this target, the Hydrologiska Byrans Vattenbalansavdelning (HBV)-light hydrological model was applied to the seven hydrological stations in the "four sources" of the Tarim River basin, and the composition of the runoff from each basin was analyzed both qualitatively and quantitatively.

2 Study area, data, and methods

2.1 Study area

The Tarim River basin covers more than 1.02 million km^2 and is located in an extremely dry region with a fragile eco-environment (Lyu et al., 2015; Su et al., 2016; Li et al., 2020). The Tarim River basin is a closed inland catchment flanked by the Tianshan and Kunlun Mountains. Nine water systems (144 rivers in total) have flowed into the mainstream Tarim River throughout history. The Tarim River mainstream has undergone significant changes as a result of disturbance from excessive human activities, especially the overexploitation of water resources (Chen et al., 2009; Lyu et al., 2015). Since the 1950s, water systems have gradually been dismembered, and only four water systems with hydraulic relationships with the mainstream remain. The Aksu River originates from the Tianshan Mountains and includes two branches (the Kumarik and Toshkan Rivers). The Yarkand River originates north of Karakoram Mountain. The Yurunkash and Karakash Rivers upstream of the Hotan River originate from the Kunlun and Karakorum Mountains, respectively, and they flow through the Taklimakan Desert from south to north before entering the mainstream of the Tarim River. The fourth source region of the Tarim River is the Kaidu-Kongque River, which supplies water to the mainstream through the Kuta Canal. The Tarim River is fed entirely by rainfall and snow/glacier melt in the four headstream regions and has no other contributors to river runoff (Chen et al., 2009; Bolch et al., 2022; Wang et al., 2021), more details of glacier information can be found in Section 2.2.3.

2.2 Data

2.2.1 Climate data

A daily gridded data set, which was developed by the China Meteorological Administration, was used as observation meteorological data. This data set applied the "anomaly approach" to interpolate to 0.25° × 0.25° based on high-density ground observation meteorological stations in China. The climatology is first interpolated by thin-plate smoothing splines, and then a gridded daily anomaly derived from the angular distance weighting method is added to climatology to obtain the final data set (Wu and Gao, 2013). The data set includes daily mean temperature and precipitation and has been widely employed in many studies assessing past climate change in China (Wu et al., 2017; Xu et al., 2018; Guo et al., 2020).

The source for the monthly potential evapotranspiration during 1961–2020 was the Climatic Research Unit (CRU) data set at a spatial resolution of 0.5°; the data were calculated based on the Penman–Monteith formula, which includes the maximum, minimum, and mean temperatures; vapor pressure; and cloud cover (Harris et al., 2014; Wang et al., 2020).

2.2.2 Hydrological data

This research selected seven hydrological stations located in the four headwater sections, and hydrological data were from the Hydrological Yearbook provided by the Ministry of Water Resources, China. The annual river runoff data for the seven hydrological stations were from 1957 to 2017, while the commonly covered period of the daily runoff data was 1964–1987, and the monthly data were from 1961 to 1999 (Table 1).

2.2.3 Geographic data

According to the most recently updated Randolph Glacier Inventory (RGI, Pfeffer et al., 2014), we extracted the glacier data of each catchment (Fig. 1). The number of

Table 1 Information on hydrological stations

Station	Longitude (E)	Latitude (N)	Daily discharge	Monthly discharge	Annual discharge
Xiehela	79°37′	41°34′	1964/1/1–1987/12/31	1957/1–2011/12	1957–2017
Shaliguilanke	78°36′	40°57′	1961/1/1–1989/12/31	1957/1–2011/12	1957–2017
Kaqun	76°54′	37°59′	1961/1/1–2011/12/31	1961/1–2011/12	1957–2017
Yuzimenleke	77°12′	37°38′	1961/1/1–2011/12/31	1961/1–2011/12	1957–2017
Tongguziluoke	79°26′	36°52′	1962/1/1–2011/12/31	1962/1–2011/12	1957–2017
Wuluwati	79°55′	36°49′	1961/1/1–1999/12/31	1961/1–1999/12	1957–2017
			2007/1/1–2011/12/31	2007/1–2011/12	
Dashankou	85°43′	42°15′	1961/1/1–2011/12/31	1961/1–2011/12	1957–2017

glaciers was from the RGI in each subcatchment, and the glacier areas were calculated by ArcGIS 10.2 (Table 2). Among the seven hydrological subcatchments, the largest proportion of glacierized area in the basin area was Tongguziluoke, at approximately 19.39%, followed by Xiehela (18.25%). Although the Kaqun subcatchment had the largest glacier area, the glacierized proportion accounted for 12.10%. The glacierized area in the Dashankou subcatchment was only 299 km^2, only accounting for 1.60% of the catchment area.

A digital elevation model with a 30 m resolution was provided by the Shuttle Radar Topography Mission (SRTM) of the National Aeronautics and Space Administration. In this study, catchment and glacierized areas were classified into different elevation zones according to the 500 m band (Fig. 2).

Table 2 Information on the glaciers (from: RGI)

	Glaciers area/km^2	Number of Glaciers	Subcatchment area/km^2
Xiehela	2366	1540	12966
Shaliguilanke	647	853	18411
Kaqun	5654	4739	46740
Yuzimenleke	294	371	5522
Tongguziluoke	2873	1546	14818
Wuluwati	1986	2279	21470
Dashankou	299	688	18636

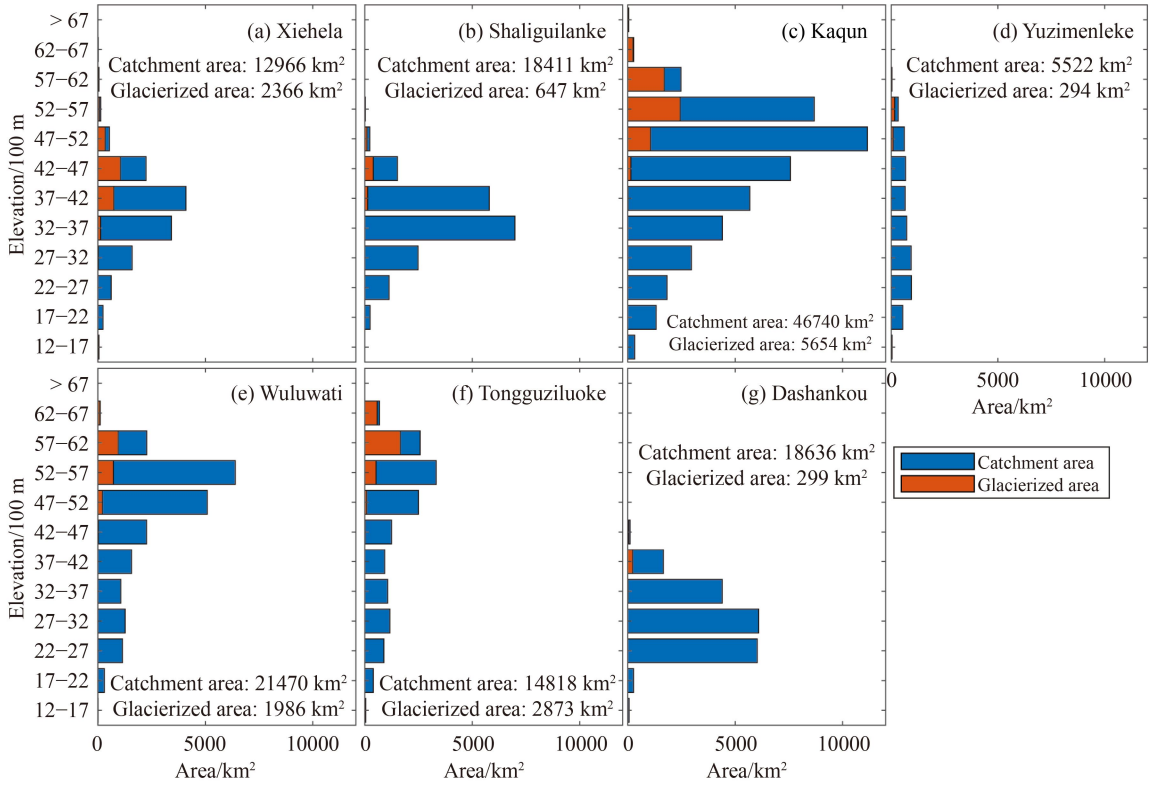

Fig. 2 Catchment area and glacierized area corresponding to different elevation zones at the headwaters of the Tarim River basin. (a) Xiehela; (b) Shaliguilanke; (c) Kaqun; (d)Yuzimenleke; (e) Wuluwati; (f) Tongguziluoke; (g) Dashankou; the bule represents the catchment area, and the red presents the glacierized area.

2.3 Methods

2.3.1 HBV-light model

The Hydrologiska Byrans Vattenbalansavdelning (HBV) model, which was initially proposed by the Swedish Meteorological and Hydrological Institute (SMHI), is a semi-distributed conceptual rainfall-runoff model (Xu et al., 2017; Ali et al., 2018). The model consists of four routines, i.e., snow, soil, response (or groundwater), and routing routines (Seibert and Vis, 2012; Etter et al., 2017; Wang et al., 2019b; Idrizovic et al., 2020). However, the original version of the HBV is not suitable for the Tarim River basin, as glacier meltwater is an important component of the hydrological processes in this area. Therefore, a modified version, named the HBV-light model (Konz and Seibert, 2010; Seibert and Vis, 2012; Xu et al., 2017; Seibert et al., 2018), in which the snowmelt routine and the glacier melt and accumulation processes were reformulated, was used in this study. The snow and glacier routine applied a degree-day method to illustrate snow and glacier melt (Seibert and Vis, 2012; Xu et al., 2017; Seibert et al., 2018). The HBV-light model simulates daily discharge with the inputs of daily precipitation, temperature and monthly potential evapotranspiration. In the process of adopting a hydrological model, the selection of runoff calibration and validation periods is a very important step. Traditionally, it is generally necessary to select the period with no missing observation data. In the process of simulating runoff by the HBV-light model, there should first be a warm-up period, and the length period of calibration and validation is generally the same.

Precipitation is considered to be either snow or rain, depending on whether the temperature is above or below a threshold temperature (TT). The amount of snowmelt water is calculated by the degree-day factor of snow (DF_{snow}) (Eq. (1)). After the completion of snowmelt, glacier melt starts by using the degree-day factor of glacier (DF_{glacier}) (Eq. (2)). Meltwater and rainfall are retained within the snowpack until they exceed a certain fraction of the water equivalent of snow. When the temperature drops below the TT, the amount of refreezing liquid water within the snowpack is computed using a refreezing coefficient (CFR) and degree-day factor ($CFMAX$) (Eq. (3)). Based on the relation between water content of the soil box (SM), its largest value (FC) and the shape coefficient ($BETA$), the sum of rainfall and meltwater $P(t)$ were divided into water filling the soil box and groundwater recharge (Eq. (4)). The actual evapotranspiration ($ETA(t)$) from the soil box equals the potential evapotranspiration ($ETP(t)$) when SM/FC is above threshold for reduction of evaporation (LP), while a linear reduction is used when SM/FC is below this value (Eq. (5)). The soil is characterized by two-level reservoirs: upper groundwater box (SUZ) and low zone box (SLZ). Only when there is water in the SUZ can it percolate into the SLZ according to the maximum percolation rate from the upper to the lower box. Runoff at the groundwater boxes ($Q_{GW}(t)$) is determined by the SUZ, threshold of the water content in the upper reservoirs (ULZ), and recession coefficients (K_0, K_1, and K_2) (Eq. (6)). The groundwater runoff is finally transformed by a triangular weighting function ($MAXBAS$) to simulate the total runoff $Q_{\mathrm{sim}}(t)$ (Eq. (7)):

$$\mathrm{Melt}_{\mathrm{snow}} = DF_{\mathrm{snow}}(T - TT), \tag{1}$$

$$\mathrm{Melt}_{\mathrm{glacier}} = DF_{\mathrm{glacier}}(T - TT), \tag{2}$$

$$\mathrm{Refreezing} = CFR \times CFMAX \times (TT - T), \tag{3}$$

$$\mathrm{recharge} = P(t) \times \left(\frac{SM(t)}{FC}\right)^{BETA}, \tag{4}$$

$$ETA(t) = ETP(t) \times \min\left(\frac{SM(t)}{FC \cdot LP}, 1\right), \tag{5}$$

$$\begin{aligned} Q_{GW}(t) &= K_1 \times SUZ + K_2 \times SLZ \\ &\quad + K_0 \times \max(SUZ - UZL, 0), \end{aligned} \tag{6}$$

$$Q_{\mathrm{sim}}(t) = \sum_{i=1}^{MAXBAS} c(i) \times Q_{GW}(t - i + 1),$$

$$\text{where, } c(i) = \int_{i-1}^{i} \left(\frac{2}{MAXBAS} - \left|u - \frac{MAXBAS}{2}\right| \times \frac{4}{MAXBAS^2}\right) \mathrm{d}u. \tag{7}$$

2.3.2 Genetic algorithm and Powell optimization

The HBV-light model was automatically calibrated using the genetic algorithm and Powell optimization method (GAP; Seibert, 2000), in which the selection of optimum parameters was done first and then fine tuning was done to further enhance the objection function. In the GAP method, the first step is to generate the optimized parameter sets by using the genetic algorithm (GA) with an evolutionary mechanism of selection and recombination of a set of initial, randomly selected parameter sets. During the second step, parameter sets are fine-tuned using Powell's quadratically convergent method as described by Press et al. (2002) (Seibert, 2000; Seibert and Vis, 2012). In this research, the settings of the GAP can be summarized as follows: number of parameter sets, 50; model runs, 5000. The total number of 5000 model runs was divided into 4000 runs for the GA and 1000 model runs for the subsequent local optimization by using Powell's quadratically convergent method.

2.3.3 Model performance evaluation

Model performance criteria were used to describe the similarity between the observed and simulated runoff in

the calibration and validation periods (Gupta et al., 2009). The criteria included the Nash-Sutcliffe efficiency (NSE), percent bias (PBIAS), root mean squared error standard deviation ratio (RSR), and Kling-Gupta efficiency (KGE).

The NSE is commonly used, in part because it normalizes model performance to an interpretable scale (Nash and Sutcliffe, 1970). The NSE ranges from negative infinity to 1 (1 inclusive). Generally, the closer to 1 the NSE is, the better the similarity between the simulations and the observations of river runoff. A negative NSE indicates unacceptable performance of the model (Moriasi et al., 2007; Gupta et al., 2009; Knoben et al., 2019).

The RSR is the ratio of the root mean square error (RMSE) and standard deviation of the measured river runoff (Legates and McCabe, 1999; Moriasi et al., 2007). The RSR includes scaling and normalization factors and incorporates the benefits of the error index (Chen et al., 2012). The closer the RSR is to 0, the better the hydrological model performance.

The PBIAS is the deviation of the data being evaluated and is defined as the percentage of the cumulative sum of observations minus the simulations to the cumulative sum of the observed runoff (Gupta et al., 2009). The optimal value is 0, positive values represent a model bias toward underestimation, whereas negative values indicate a bias toward overestimation (Moriasi et al., 2007; Gupta et al., 2009; Chen et al., 2012).

The KGE was proposed to unify three scaling factors: correction, bias, and variability, and to define the lower limits of the three components. The KGE can considerably improve the bias and variability measurements and may slightly decrease the correlation (Gupta et al., 2009; Kling et al., 2012).

2.3.4 Sensitivity analysis

To assess the impact of the observed climate changes on runoff changes, three additional sensitivity experiments were designed in this study to quantify the isolated effects of temperature and precipitation on runoff changes in the Tarim River basin. The first sensitivity test was based on the observed precipitation and detrended temperature, the second sensitivity test was based on the detrended precipitation and observed temperature, and the last sensitivity test applied the detrended precipitation and the detrended temperature, which set a background climatic condition after removing the effects of climate change.

Climatic variables with significant trends were detrended, following the method proposed by Bouraoui et al. (2004) and Wang et al. (2015):

$$T_{\text{detrend}} = T - \beta_T \times (t_x - t_0), \tag{8}$$

$$P_{\text{detrend}} = P \times (P_m - \beta_P \times (t_x - t_0))/P_m, \tag{9}$$

where T_{detrend} and T are the detrended and observed daily temperatures, respectively; P_{detrend} and P are the detrended and observed daily precipitation values, respectively; P_m is the observed monthly precipitation; β_T and β_P are the Sen's slope values for monthly temperature and precipitation, respectively; t_0 is the base year; and t_x is the current year. The detrended daily temperature and precipitation were assumed to be the background climatic conditions after removing the effects of climate change.

2.3.5 Thickness of the glacier

The Glacier Bed Topography version 2 (GlabTop2) model is an advanced version of the GlabTop mode, which is a model used for assessing the spatial distribution of ice thickness by estimating glacier depths. A brief description of the model is given in this section; for more details, readers can refer to Frey et al. (2014).

The ice thickness calculation with GlabTob2 requires estimating the basal shear stress (τ) and the shape factor f. Based on these two parameters and Eq. (10), the volume based on the mean ice thickness along the central flowline h_f was calculated:

$$h_f = \frac{\tau}{f\rho g \sin(\alpha)}, \tag{10}$$

where τ is the average basal shear stress along the central flowline calculated using Eq. (11), g is the gravitational acceleration (9.8 $\text{m}\cdot\text{s}^{-1}$), α is the mean surface slope, and ρ is the density of ice (900 $\text{kg}\cdot\text{m}^{-3}$). f is a dimensionless shape factor that accounts for drag by valley walls and glacier beds. f was chosen to be a constant of 0.8, which is considered the typical value for valley glaciers.

The value of basal shear stress τ (in kPa) was estimated from an empirical relation between τ and glacier elevation range ΔH (in km) proposed by Haeberli and Hoelzle (1995) as given in Eq. (11):

$$\tau(\text{kPa}) = \begin{cases} 0.5 + 159.8\Delta H - 43.5(\Delta H)^2, & \Delta H \leqslant 1.6\ \text{km} \\ 150, & \Delta H > 1.6\ \text{km} \end{cases}. \tag{11}$$

To obtain the glacier volume for each elevation zone, the thickness of the glacier was deduced by the GlapTop2 model (Linsbauer et al., 2012; Frey et al., 2014), and the results are shown in Fig. 3. The glacier volume was 244.54 km^3 in the Aksu subbasin, 410.69 km^3 in the Yarkand subbasin and 417.68 km^3 in the Hotan River subbasin. The volume was only 10.00 km^3 in the Kaidu-Kongque River subbasin.

3 Results

3.1 Changes in temperature, precipitation and runoff

Changes in temperature, precipitation and runoff during 1961–2016 in the four source regions in the Tarim River basin are shown in Fig. 4. In the Aksu River subbasin, the annual mean temperature was –3.47°C and showed a

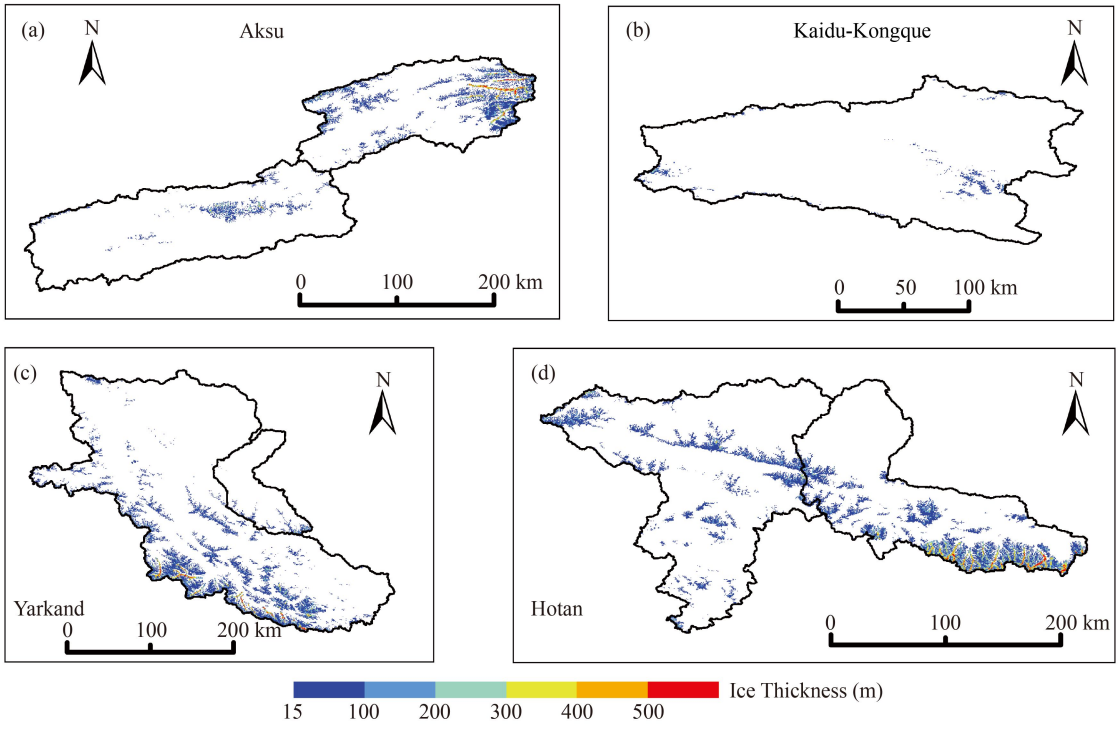

Fig. 3 Spatial distribution of ice thickness of the four subbasin in the Tarim River basin. (a) Aksu River subbasin; (b) Kaidu-Kongque River subbasin; (c) Yarkand River subbasin; and (d) Hotan River subbasin.

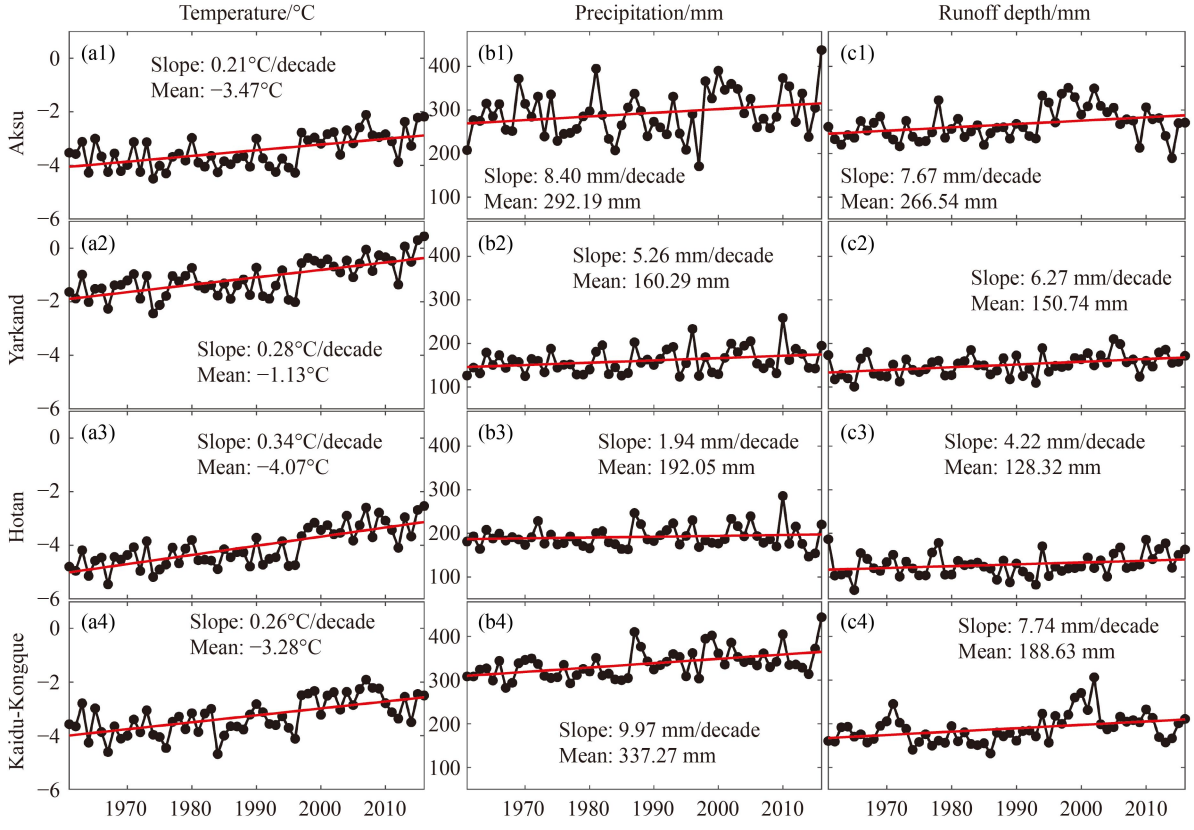

Fig. 4 Changes in annual mean temperature, annual precipitation and runoff depth in the Aksu (a1, b1, and c1), Yarkand (a2, b2, and c2), Hotan (a3, b3, and c3), and Kaidu-Kongque (a4, b4, and c4) River subbasins during 1961–2016 (red lines represent the linear trends).

significant warming rate of 0.21°C per decade (Fig. 4(a1)); the annual precipitation was approximately 292.19 mm and showed a nonsignificant increase of 8.40 mm per decade (Fig. 4(b1)); the total annual runoff depth at the Xiehela and Shaliguilanke hydrological stations was approximately 266.54 mm (Fig. 4(c1)), which showed no significant trend before the mid-1990s but clearly increased thereafter. The annual runoff depth showed a significant increase of 7.67 mm per decade, and the correlation coefficient with temperature was higher than that with precipitation.

In the Yarkand River subbasin, the annual mean temperature and annual precipitation were –1.13°C and 160.29 mm, respectively. The annual mean temperature significantly increased at a rate of 0.28°C per decade, while the annual precipitation non-significantly increased at a rate of 5.26 mm per decade (Figs. 4(a2) and 4(b2)). The annual runoff depth in the Yarkand River basin (total annual runoff depth from the Kaqun and Yuzimenleke hydrological stations) was 150.74 mm, which significantly increased at a rate of 6.27 mm per decade (Fig. 4(c2)). The annual runoff depth was significantly correlated with the annual mean temperature during 1961–2016 but was not significantly correlated with the annual precipitation.

The annual mean temperature in the Hotan River subbasin was –4.07°C during 1961–2016, which significantly increased at a rate of 0.34°C per decade (Fig. 4(a3)). Moreover, the annual precipitation was approximately 192.05 mm, with an increasing trend (1.94 mm per decade) that was not statistically significant (Fig. 4(b3)). The annual runoff depth was approximately 128.32 mm, and it non-significantly increased at a rate of 4.22 mm per decade (Fig. 4(c3)). The annual runoff depth was significantly positively correlated with temperature with a coefficient of 0.65 (p<0.01) but had no significant correlation with precipitation.

In the Kaidu-Kongque River subbasin, the annual mean temperature was –3.28°C, and it significantly increased at a rate of 0.26°C per decade during 1961–2016 (Fig. 4(a4)), while the annual precipitation was 337.27 mm, and it significantly increased at a rate of 9.97 mm per decade (Fig. 4(b4)). The annual runoff depth at the main gauging station, Dashankou, was 188.63 mm, which significantly increased at a rate of 7.74 mm per decade (Fig. 4(c4)). The relationships between annual runoff depth and precipitation and temperature were both significantly positive, but a higher correlation of 0.62 was detected with precipitation than that of 0.49 with temperature.

Runoff in the Aksu, Yarkand, and Hotan River subbasins was more sensitive to changes in temperature than to changes in precipitation, which means that meltwater has a large contribution to the total runoff depth; moreover, the relationship between runoff and precipitation was much higher than that with temperature in the Kaidu-Kongque River subbasin, which means that runoff is fed mainly by precipitation.

3.2 Performance of the hydrological model

Precipitation includes liquid rainfall and solid snow; in order to more accurately distinguish composition of rainfall and snowmelt in river runoff, this paper applied the HBV-light model to deconstruct runoff into three parts, i.e., rainfall, snowmelt, and glacier melt, to quantify the proportion of each part to the total runoff.

The HBV-light model was calibrated and validated satisfactorily with a set of parameters that could represent the hydrological characteristics of the seven gauging stations in the Tarim River basin. The performances of the HBV-light model on the daily scales during the calibration (1964–1975) and validation (1976–1987) periods for each hydrological station are shown in Fig. 5. The comparison of observed and simulated monthly and annual discharge during the calibration and validation periods for each hydrological are shown in Supplementary Materials. A summary of the NSE, KGE, RSR, and PBIAS for the daily and monthly runoff simulation results is shown in Tables 3 and 4.

At the daily scale, the NSE was greater than 0.60 and the KGE was greater than 0.70 at all stations, while the RSR was approximately 0.50, and the PBIAS was within 10% at all seven stations (Table 3). At the monthly scale, the NSE and KGE were higher than 0.80 at all hydrological stations and even above 0.90 at some stations. The RSR was approximately 0.30, which was lower than the daily value. The monthly PBIAS was the same as that for the daily scale (Table 4). The results mean that the HBV-light model had a very good performance rating the during calibration and validation periods, which was recommended by Moriasi et al. (2007). The HBV-light model clearly had a good simulation ability for the inland river basins fed by both meltwater and precipitation.

To further describe the simulation ability of the hydrological model for extreme river discharge, we compared the 90th percentile of river runoff between the observations and simulations by the HBV model in the calibration and validation periods (Fig. 6). The results showed that the 90th percentile of the HBV hydrological model-simulated runoff was slightly higher than the observed values at the Xiehela, Kaqun, Yuzimenleke, Tongguziluoke, and Wuluwati stations, and it was slightly lower than the observed values at the Shaliguilanke and Dashankou stations. Finally, all the gaps between calibration and validation at each station were less than 0.50 mm.

3.3 Runoff composition at the annual scale

In the Aksu River subbasin, multiple annual average runoff depths from rainfall, snowmelt, and glacier melt were 89.85, 74.40, and 89.56 mm, respectively, accounting for 35.40%, 29.31%, and 35.29% of the total annual runoff. Snowmelt and glacier melt, which were determined mostly by temperature, composed 64.71% of the total

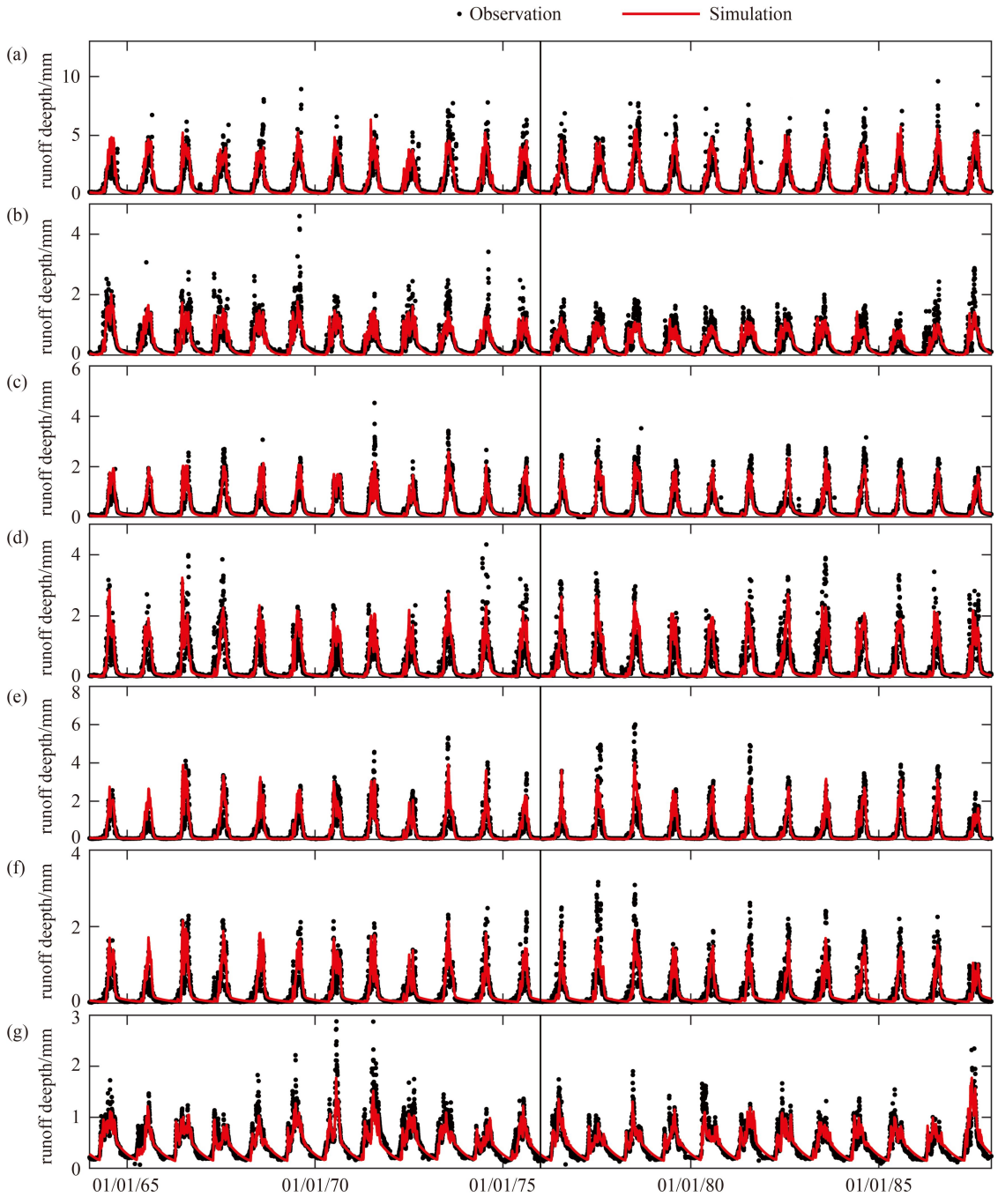

Fig. 5 Observed and simulated daily discharge by the HBV-light model for 1964–1987 at each hydrological station (calibration period: 1964–1975; validation period: 1976–1987; (a) Xiehela; (b) Shaliguilanke; (c) Kaqun; (d)Yuzimenleke; (e) Wuluwati; (f) Tongguziluoke; (g) Dashankou).

runoff. The interannual variation in glacier meltwater showed that its proportion to the total runoff was the highest in 1997 at 51.37% but the lowest in 1964 at only 24.78%. In terms of rainfall and snowmelt, their proportions to total runoff were 46.61% in 2012 and 39.90% in 1979; additionally, the values were highest at 21.13% in 1984 and lowest at 17.76% in 2007 (Fig. 7(a)).

Glacial meltwater accounted for a major portion of runoff in the Yarkand and Hotan River subbasins. The annual glacier meltwater runoff depths were 63.95 and 69.95 mm, respectively, which accounted for 46.72% and 58.73% of the runoff in the Yarkand and Hotan River subbasins. The proportions of rainfall to runoff ranked second in both the Yarkand and the Hotan River subbasins, accounting for 35.01% and 31.07%, respectively. The snowmelt volumes in the two subbasins were 25.00 and 12.14 mm, accounting for 18.27% and 10.20% of the runoff, respectively (Figs. 7(b) and 7(c)).

Table 3 Performance of the HBV-light model at the daily scale in the Tarim River basin for the calibration and validation periods

Station	Calibration				Validation			
	NSE	KGE	RSR	PBIAS	NSE	KGE	RSR	PBIAS
Xiehela	0.72	0.85	0.53	8.81%	0.78	0.89	0.47	−0.09%
Shaliguilanke	0.75	0.84	0.50	−7.84%	0.71	0.80	0.54	−10.32%
Kaqun	0.84	0.90	0.39	−1.19%	0.89	0.89	0.32	−8.18%
Yuzimenleke	0.66	0.83	0.58	6.92%	0.75	0.86	0.50	−5.34%
Tongguziluoke	0.67	0.83	0.57	8.96%	0.77	0.87	0.48	−2.70%
Wuluwati	0.70	0.83	0.55	9.57%	0.79	0.83	0.46	−8.69%
Dashankou	0.76	0.77	0.49	−7.45%	0.74	0.76	0.51	3.76%

Table 4 Performance of the HBV-light model at the monthly scale in the Tarim River basin for the calibration and validation periods

Station	Calibration				Validation			
	NSE	KGE	RSR	PBIAS	NSE	KGE	RSR	PBIAS
Xiehela	0.85	0.87	0.38	8.81%	0.91	0.91	0.30	−0.09%
Shaliguilanke	0.88	0.88	0.34	−7.84%	0.82	0.86	0.42	−10.32%
Kaqun	0.89	0.90	0.33	−1.19%	0.95	0.89	0.22	−8.18%
Yuzimenleke	0.84	0.88	0.39	6.92%	0.90	0.86	0.31	−5.34%
Tongguziluoke	0.82	0.88	0.43	8.96%	0.92	0.92	0.28	−2.70%
Wuluwati	0.84	0.88	0.40	9.57%	0.92	0.90	0.28	−8.69%
Dashankou	0.84	0.82	0.40	−7.45%	0.83	0.81	0.42	3.76%

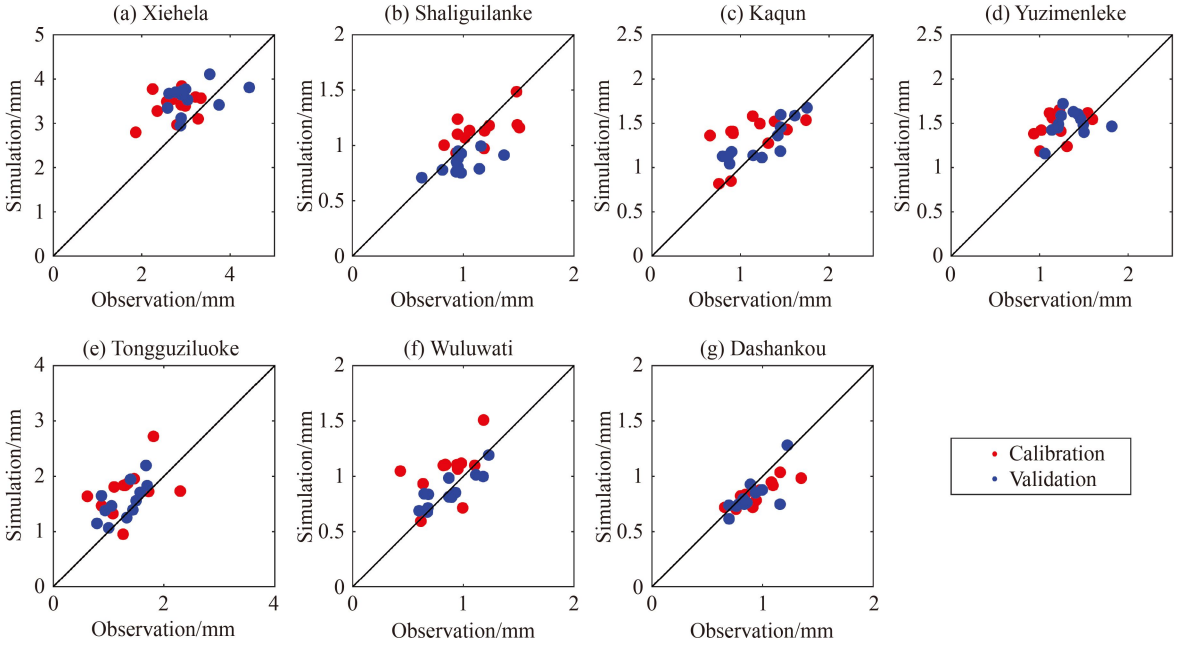

Fig. 6 Comparison of 90th percentile runoff between observed and simulated discharge at each hydrological station in the calibration and validation periods. The red dot represent the calibration period, and the bule dot represent validation period.

Compared with the other three subbasins, the runoff composition from the Kaidu-Kongque River had different characteristics, where glacierized areas made up only 1.6% of the catchment area. Runoff generated by rainfall was 147.33 mm annually, accounting for 80.86% of the runoff, while runoff generated by snowmelt was 34.87 mm, accounting for 19.14% of the runoff. The proportion of rainfall to the total runoff was the lowest in 1988 (approximately 71.67%) and the highest (86.30%) in 2007. The highest or lowest proportions from snowmelt occurred in the year when the rainfall proportion was the lowest or the highest (Fig. 7(d)).

For the four subbasins, the portions of annual runoff in the Tarim River basin during 1961–2016 that were generated from rainfall, snowmelt, and glacier melt were 67.93, 34.15, and 62.72 mm, respectively, accounting for 41.22%, 20.72%, and 38.06% of river runoff, respectively. Snowmelt and glacier melt, which were affected mostly by temperature changes, contributed 58.78% to river runoff.

Glaciers can withstand extreme water shortages, as the supply of glacier meltwater can be sustained during dry years with reduced precipitation and storage (Pritchard, 2019). More precipitation in wetter years forms a thick snowpack on the surfaces of ice/glaciers, which increases snow albedo and results in slow snow/ice melt (Zhao et al., 2013). To quantify the regional response, the average effects in five dry years with comparatively lower than normal precipitation and in five wet years with comparatively higher than normal precipitation were compared to show the different contributions of glacier meltwater to the annual runoff in the Tarim River Basin (Table 5). For Aksu, the dry years were 1975, 1983, 1984, 1995, and 1997; in contrast, the wet years were 1969, 1981, 2000, 2010, and 2016. For Yarkand, the dry years were 1970, 1979, 1997, 1994, and 1985; the wet

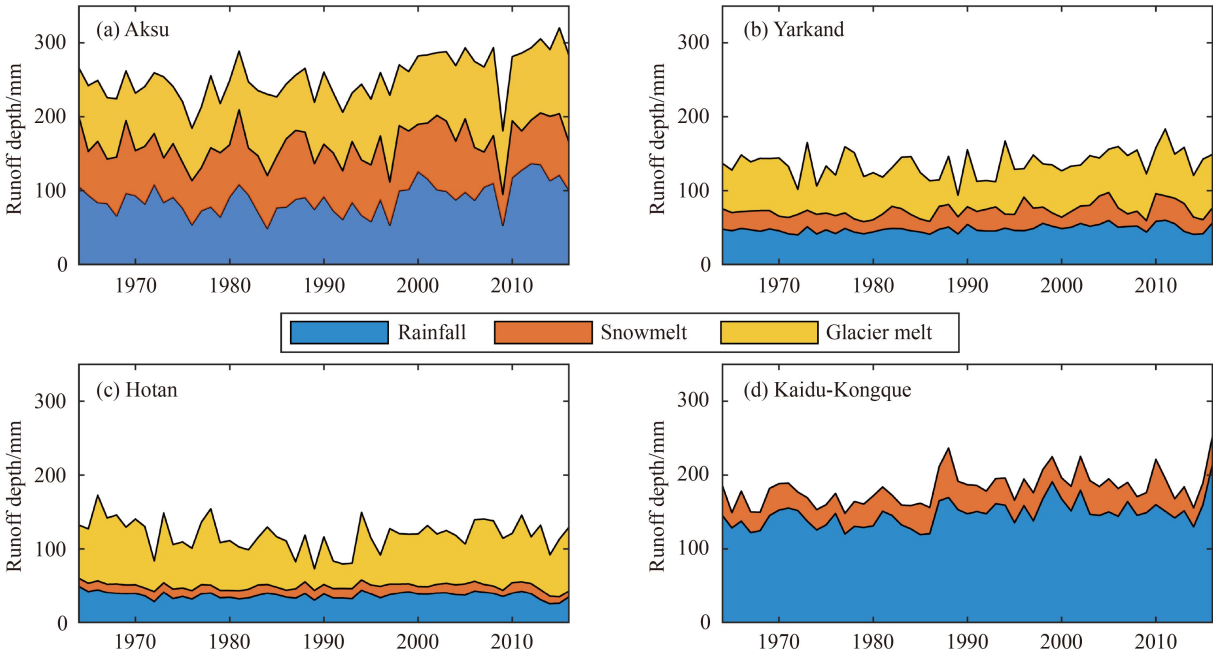

Fig. 7 Annual runoff generated by rainfall, snowmelt, and glacier melt during 1961–2016.

Table 5 Proportion of glacier meltwater in runoff in dry and wet years

	Aksu	Yarkand	Hotan	Tarim
Dry years	42.74%	52.95%	62.28%	41.20%
Wet years	31.67%	35.88%	50.74%	33.05%

years were 1987, 1996, 2002, 2005, and 2010. Dry years in the Hotan were 1963, 1985, 1986, 2014, and 2015; in contrast, the wet years were 1987, 1996, 2002, 2005, and 2010. For the whole Tarim River basin, the dry years were 1975, 1984, 1985, 1997, and 2014; in contrast, the wet years were 1981, 1987, 2002, 2010 and 2016.

Glacial meltwater contributed 42.74% to the annual runoff in dry years, which was 7.76% higher than the multiple-year average and 11.07% higher than wet years in the Aksu River subbasin. Glacial meltwater accounted for 52.95% and 35.88% of the total runoff in dry and wet years in the Yarkand River subbasin, respectively, and accounted for 62.28% and 50.74% in the Hotan River subbasin, respectively. In the Tarim River basin overall, glacier meltwater contributed 41.20% to the total runoff in dry years and 33.05% in wet years.

3.4 Seasonal cycle of runoff components

The distribution of the monthly runoff contributed by rainfall, snowmelt, and glacier melt in the four subbasins of the Tarim River basin during 1961–2016 is shown in Fig. 8. The effects of temperature and precipitation changes on snowmelt runoff varied seasonally. Snow melted mainly from April to October in the four subbasins, with the maximum melt occurring in June or July. Snow seldom melted in the winter months. Glaciers melted from April to September, with a peak in July or August, which was later than the peak of snowmelt. The seasonal distribution of runoff generated by rainfall, snowmelt, and glacier melt is shown in Table 6.

In the Aksu River subbasin, snowmelt was the dominant component in spring and winter, accounting for 56.79% and 48.33%, respectively. The dominant runoff component in summer was glacier meltwater, which accounted for 38.36%, and rainfall accounted for 36.43%. In autumn, rainfall, snowmelt, and glacier melt runoff accounted for 39.24%, 19.80%, and 40.96%, respectively.

Runoff generated by rainfall in the Yarkand River subbasin was the dominant component in spring, autumn, and winter, accounting for 45.34%, 44.22%, and 57.60%, respectively. Snowmelt runoff ranked second in spring and winter, accounting for 40.81% and 42.33% of the total runoff, respectively. Glacial melt runoff was dominant in summer, accounting for 54.70%, while it was negligible in winter.

The interannual distribution of runoff compositions in the Hotan River subbasin was similar to that in the Yarkand River subbasin in that there was no glacier meltwater in winter. In spring, autumn, and winter, rainfall runoff was the dominant component of the total runoff, accounting for 57.58%, 50.60%, and 71.12%, respectively. Glacial meltwater was the dominant component in summer, accounting for 69.71% of the total runoff.

Glacial meltwater in the Kaidu-Kongque River basin was negligible. Runoff contributed by rainfall was the dominant component in the four seasons, accounting for 74.05%, 80.47%, 85.39%, and 84.82% of the seasonal runoff, and the remaining part of the surface runoff was

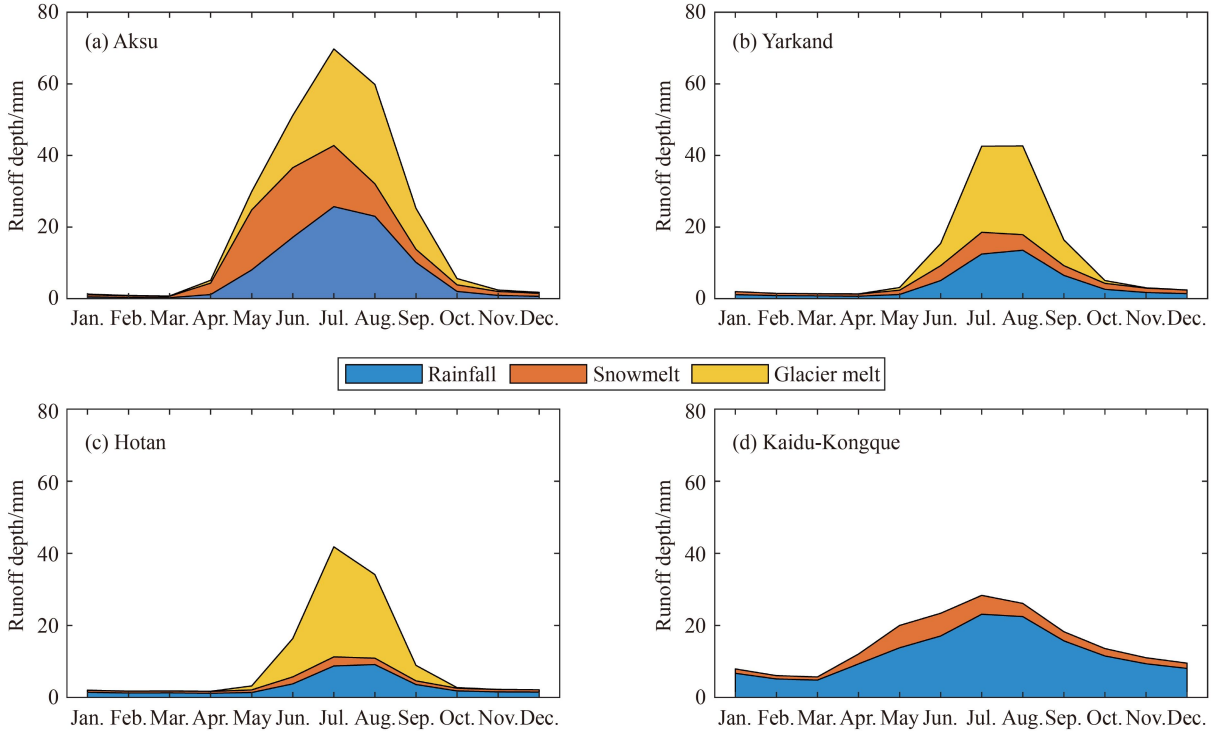

Fig. 8 Interannual distribution of runoff generated by rainfall, snowmelt, and glacier meltwater in the (a) Aksu, (b) Yarkand, (c) Hotan, and (d) Kaidu-Kongque River subbasins during 1961–2016.

Table 6 Seasonal distribution of runoff components in the Tarim River basin

River Basin		Spring /mm	Summer /mm	Autumn /mm	Winter /mm
Aksu	Rainfall	9.45	65.87	13.06	1.47
	Snowmelt	20.34	45.57	6.59	1.89
	Glacier melt	6.02	69.34	13.63	0.55
Yarkand	Rainfall	2.63	31.06	10.84	3.38
	Snowmelt	2.37	14.55	5.60	2.49
	Glacier melt	0.80	55.06	8.08	0.00
Hotan	Rainfall	3.92	21.74	7.07	4.28
	Snowmelt	1.76	6.22	2.42	1.74
	Glacier melt	1.13	64.34	4.47	0.00
Kaidu-Kongque	Rainfall	28.01	62.65	36.66	20.01
	Snowmelt	9.82	15.21	6.27	3.58
	Glacier melt	–	–	–	–
Tarim	Rainfall	7.93	40.75	13.83	5.42
	Snowmelt	7.28	19.48	5.08	2.30
	Glacier melt	1.96	53.32	7.31	0.13

from snowmelt.

In the Tarim River basin overall, runoff generated by rainfall was the dominant component in spring, autumn and winter, accounting for 46.21%, 52.74%, and 65.05%, respectively. Snowmelt ranked second in spring and winter, accounting for 42.40% and 29.33%, respectively. Glacial melt runoff was the dominant component in summer, accounting for 46.96% of the total runoff, while it accounted for only 1.62% in winter.

3.5 Quantitative effect of climate drivers on runoff changes

River runoff in the Tarim River basin has significantly increased in recent decades due to increasing temperature and precipitation. Runoff in the Aksu, Yarkand, and Kaidu-Kongque River subbasins has increased significantly, while runoff in the Kaidu-Kongque River has non-significantly increased.

Sensitivity analyses showed that annual river runoff in the Aksu River basin would have been 225.98 mm under a scenario in which temperature and precipitation varied without anthropogenic forcing (P_{detrend}, T_{detrend}) during 1961–2016, i.e., 27.82 mm less than the observed value. This difference can be deconstructed into 12.36 mm caused by rising temperatures and 15.46 mm caused by increasing precipitation. These values indicate that river runoff increased by 12.29% due to regional climate change under the background of global warming, and the contributions of temperature and precipitation changes to increased runoff were 55.56% and 44.44%, respectively (Table 7). For the two tributaries, climate change resulted in runoff increases of 12.53% (44.10 mm) and 11.86% (16.28 mm) from the Kumarik and Toshkan Rivers, respectively. Rising temperatures contributed 69.11% to the increase in runoff from the Kumarik River and –2.62% to the increase in runoff from the Toshkan River.

Table 7 Results of sensitivity analyses: the influence of temperature and precipitation changes on runoff and runoff composition in the Tarim River basin (mm)

River Basin	Test	River runoff	By rainfall	By snowmelt	By glacier melt
Aksu	P, T	253.80	89.85	74.40	89.56
	P, $T_{detrend}$	241.41	84.61	74.32	82.48
	$P_{detrend}$, T	238.32	84.17	68.05	86.10
	$P_{detrend}$, $T_{detrend}$	225.98	79.01	68.40	78.57
Yarkand	P, T	136.87	47.92	25.00	63.95
	P, $T_{detrend}$	128.39	45.42	25.81	57.16
	$P_{detrend}$, T	132.49	44.83	24.17	63.48
	$P_{detrend}$, $T_{detrend}$	124.07	42.44	24.83	56.79
Hotan	P, T	119.10	37.01	12.14	69.95
	P, $T_{detrend}$	99.74	33.14	12.63	53.97
	$P_{detrend}$, T	118.39	36.49	11.93	69.97
	$P_{detrend}$, $T_{detrend}$	99.00	32.62	12.41	53.96
Kaidu-Kongque	P, T	182.20	147.33	34.87	0.00
	P, $T_{detrend}$	185.46	146.94	38.52	0.00
	$P_{detrend}$, T	161.04	132.90	28.14	0.00
	$P_{detrend}$, $T_{detrend}$	163.91	132.63	31.28	0.00
Tarim	P, T	164.79	67.93	34.15	62.72
	P, $T_{detrend}$	154.15	64.73	35.05	54.37
	$P_{detrend}$, T	156.60	63.40	31.44	61.77
	$P_{detrend}$, $T_{detrend}$	145.94	60.28	32.31	53.34

Notes: P means precipitation, $P_{detrend}$ means precipitation after detrending, T means temperature, and $T_{detrend}$ indicates the temperature after detrending.

In contrast, precipitation contributed 30.89% and 102.62% to increased runoff from the Kumarik and Toshkan Rivers, respectively. The Kumarik catchment was mainly impacted by temperature, while the Toshkan catchment was controlled by precipitation. The large difference in the temperature contributions in the two adjacent tributaries can be explained by the different glacier coverages, which were 2366 km^2 (18.25%) and 647 km^2 (3.53%) in the Kumarik and Toshkan Rivers, respectively.

The observed annual runoff was 136.87 mm in the Yarkand River subbasin during 1961–2016, and climate change contributed to an increase in runoff of 10.31% (12.80 mm). Regional temperature and precipitation changes resulted in increases in runoff of 8.44 and 4.36 mm, indicating that their contributions were 66.10% and 33.90%, respectively (Table 7). At the Kaqun station, changing temperatures led to a 9.42 mm increase in runoff, and precipitation changes led to a 4.13 mm increase. At the Yuzimenleke station, an increase in runoff of 5.88 mm was primarily caused by a precipitation increase.

In the Hotan River subbasin, the observed annual runoff was 119.10 mm during 1961–2016, which was 20.10 mm higher than the runoff under the assumption of no anthropogenic climate change. The increases in regional temperature and precipitation caused by anthropogenic forcing resulted in increases in runoff of 19.36 and 0.74 mm, respectively, which indicated that the contributions of temperature and precipitation to runoff increases were 96.32% and 3.68%, respectively. For the Yurunkash River and Karakash River, temperature contributed 98.77% and 92.12% to the runoff increase, and precipitation contributed 1.23% and 7.88%, respectively (Table 7).

In the Kaidu-Kongque River subbasin, the annual runoff was 182.20 mm, of which 163.91 mm was generated by the natural climate and 18.29 mm was contributed by climate change. There was no glacier melt runoff in the Kaidu-Kongque River subbasin, where increasing temperature and evapotranspiration finally resulted in a decrease in runoff of 2.81 mm, but increased precipitation resulted in an increase in runoff of 21.10 mm. Temperature contributed –15.39% to the runoff increase, while precipitation contributed 115.39% (Table 7).

In the Tarim River basin overall, the observed annual runoff of 18.85 mm was higher than that without anthropogenic climate change. Temperature and precipitation changes contributed 10.65 mm (56.49%) and 8.20 mm (43.51%), respectively. These values indicated that in the Tarim River basin, the effect of temperature on runoff was higher than the effect of precipitation on runoff.

In the seasonal attribution analysis (Table 8), we found that in spring, the increase in runoff in the Tarim River basin was mainly caused by precipitation, and the contribution was 73.39%. Among the four subbasins, the increase in runoff in the Aksu subbasin was the result of both temperature and precipitation, and the contribution of precipitation was higher than that of temperature. In the Kaidu-Kongque River subbasin, the contribution of temperature to the increase in runoff was negative, and the increase in runoff was entirely caused by the increase in precipitation. In the Yarkand River subbasin and Hotan River subbasin, the increase in runoff was caused by the increase in temperature and precipitation, but the contribution of temperature was higher than that of precipitation.

In summer and autumn, the contribution of temperature and precipitation to the increase in runoff were almost the same in the Aksu River subbasin, while in the Yarkand River and Hotan River subbasins, the contribution of temperature to the increase in runoff was greater than that of precipitation. For the Kaidu-Kongque River subbasin, precipitation was the main factor causing the increase in runoff. In the Tarim River basin, the contributions of temperature to runoff increase were 61.60% and 64.12%, respectively, while the contributions of precipitation were 38.40% and 35.88%.

In winter, the contribution of temperature to the increase in runoff was negative in the Aksu and Yarkand River subbasin, while in the Hotan and Kaidu-Kongque River subbasins, the contribution of precipitaiton to the increase in runoff was greater than that of temperature.

Table 8 Results of sensitivity analyses: the influence of temperature and precipitation changes on seasonal runoff depth in the Tarim River basin (mm)

River Basin	Test	Spring /mm	Summer /mm	Autumn /mm	Winter /mm
Aksu	P, T	35.82	180.78	33.29	3.92
	P, $T_{detrend}$	34.02	172.94	30.48	3.98
	$P_{detrend}$, T	32.48	171.06	31.27	3.51
	$P_{detrend}$, $T_{detrend}$	30.76	163.11	28.50	3.61
Yarkand	P, T	5.81	100.67	24.52	5.87
	P, $T_{detrend}$	5.31	94.28	22.73	6.07
	$P_{detrend}$, T	5.53	97.97	23.47	5.52
	$P_{detrend}$, $T_{detrend}$	5.02	91.74	21.64	5.67
Hotan	P, T	6.82	92.29	13.96	6.02
	P, $T_{detrend}$	6.16	76.05	11.53	6.00
	$P_{detrend}$, T	6.69	92.02	13.79	5.89
	$P_{detrend}$, $T_{detrend}$	6.04	75.72	11.38	5.86
Kaidu-Kongque	P, T	37.82	77.86	42.93	23.59
	P, $T_{detrend}$	38.83	80.77	42.57	23.29
	$P_{detrend}$, T	31.68	65.19	41.23	22.94
	$P_{detrend}$, $T_{detrend}$	32.70	67.46	41.03	22.73
Tarim	P, T	17.17	113.55	26.22	7.85
	P, $T_{detrend}$	16.54	105.50	24.22	7.89
	$P_{detrend}$, T	15.46	108.55	25.09	7.50
	$P_{detrend}$, $T_{detrend}$	14.84	100.44	23.11	7.55

Notes: P means precipitation, $P_{detrend}$ means precipitation after detrending, T means temperature, and $T_{detrend}$ indicates the temperature after detrending.

Contribution of precipitation to runoff increase in the Tarim River basin was 115.32%, while the increase in temperature to runoff was −15.32%. The increase in winter runoff in the four sources was mainly due to the increase in precipitation.

4 Discussion

As many previous studies have focused on tributaries of the Aksu River subbasin, we compared our results with existing results. Our study revealed that glacier melt accounted for 36.24% of the runoff in the Kumarik River, which was close to the results of Duethmann et al. (2015) and Ji et al. (2019), who found that the proportions of glacier melt were 35%–48% and 30%–48%, respectively; however, the value in this study was slightly higher than that discovered by Li et al. (2020), whose estimation of the contribution of glacier melt to runoff was 28.2%. In the Toshkan River, rainfall was the main component of runoff, with a proportion of 41.81%. The results by Zhao et al. (2013) also showed that the contribution percentage of rainfall was the highest, with an even higher value of 50.9%. However, Chen et al. (2019) found that runoff from glacier meltwater in the Kumarik River accounted for 59% of runoff during July–August (which was higher than our result of 39.90%) and was 39% at the Toshkan River (which was lower than our result of 44.32%).

Our research aimed to systematically quantify the dominant climate factors in the Tarim River basin. In the Aksu River subbasin, changes in regional temperature and precipitation due to global warming contributed 55.56% and 44.44% to the increases in runoff, respectively. Temperature affected runoff more than precipitation in the Yarkand and Hotan River subbasins, contributing 66.10% and 96.32%, respectively, to the total runoff increase, while precipitation contributed 33.90% and 3.68%, respectively. In the Kaidu-Kongque River subbasin, the increase in runoff was entirely caused by rising precipitation, while temperature contributed was negative to the change in runoff. According to Wang et al. (2021), who applied the Glacier-enhanced SWAT model to quantify the dominant climate factors and applied them to runoff changes in the Aksu, Yarkand and Hotan Rivers, rising temperatures contributed 66%, 13%, and 94% to the changes in runoff in these basins, respectively. The results from these two studies reached consistent findings for the Hotan and Aksu River subbasins, but there was an obvious gap in the results for the Yarkand River subbasin. Another study on the Aksu and Kaidu-Kongque River subbasins showed that the contributions of precipitation and temperature to river runoff were 35.99% and 64.01% and 55.79% and 44.21%, respectively; this study applied an integrated approach (Wang et al., 2018, 2019a).

The large uncertainties were mainly from data, hydrological models, and parameterization processes. Precipitation data are vital for hydrological modeling. Due to the complexities of terrain and topography, the accurate estimation of precipitation in high mountainous areas is still a scientific problem. Meteorological stations are sparsely distributed in the Tarim River basin and are mainly located in the low elevation zone rather than at higher altitudes. Although temperature and precipitation at high elevations were adjusted based on the temperature lapse rate and precipitation gradient, it is not clear what other factors can affect temperature and precipitation in high elevation regions. More accurate climate observations in higher elevation areas could reduce these uncertainties. In addition, through the modeling processes, small uncertainties can accumulate into considerable uncertainty (Seiller and Anctil, 2014; Li et al., 2015, 2020; Wang et al., 2021; Xin et al., 2021).

With regard to the research methods, some limitations need to be acknowledged. For hydrological modeling calibration, recent research has shifted toward multi-objective calibration from only daily discharge calibration (Duethmann et al., 2015; Ji et al., 2019). As the global temperature continues to increase, the four source regions in the Tarim River basin are expected to respond differently in terms of climate and hydrology, and the

sensitivity of the basins to future climate change under different warming scenarios needs to be studied further. In addition to temperature and precipitation, river runoff is influenced by other climate variables (Fonley et al., 2019; Fan et al., 2021). As few meteorological stations are located in high mountainous regions, this research considers only temperature and precipitation. We regretfully admit that we did not consider permafrost in our research. Under the background of global warming, changes in permafrost will significantly affect the changes in the underlying surface in high-mountain areas, and changes in permafrost and its freezing thawing process will further affect the physical, chemical, and biological processes of ecology and hydrological systems in cold regions. Therefore, in future research, we will further consider the role of permafrost in the Tarim River basin.

The runoff of the Tarim River basin showed an increasing trend, and the increase in runoff in spring was more contributed by precipitation, while in summer and autumn, the contributions of precipitation and temperature to the increase in runoff were basically the same. This result indicates that the Tarim River basin may have a risk of flooding in the future. Our results showed that the proportion of glacier melt and snowmelt to river runoff accounted for more than 50%, which increased the runoff in the short-term and supplemented water resources. In the short-term, we should seize the favorable opportunity of the increase of the water resources in the Tarim River basin to expand the scale of agricultural planting and improve the local social and economic development. However, there is no denying that climate change is a double-edged sword. The increase of runoff in the Tarim River basin is mainly caused by the glacier melt and snowmelt water. With the continuous rise of global temperature, the limited glaciers and snow in the Tarim River basin will eventually vanish, and may face a serious water shortage in the future.

5 Conclusions

The current study selected the Tarim River basin, the largest endorheic drainage system dominated by an arid inland climate, as the target area, where temperature and precipitation have increased in the last several decades. This study adopted the HBV-light hydrological model to delineate runoff in a glacierized basin. The proportions of runoff components to the total runoff were estimated annually and seasonally. We quantitatively attributed the effects of precipitation and temperature changes on runoff increases in the "four sources" of the Tarim River basin.

1) The runoff in the Aksu, Yarkand, and Hotan River subbasins was controlled by temperature, while the runoff in the Kaidu-Kongque River subbasin was controlled by precipitation because it is an area with few glaciers.

2) During 1961–2016, river runoff in the Tarim River basin generated from rainfall, snowmelt, and glacier melt, accounting for 41.22%, 20.72%, and 38.06%, respectively. Among the four subbasins, glacial meltwater was the main source in the Hotan and Yarkand River subbasins, while rainfall was the main source in the Kaidu-Kongque River subbasin. And the three types water source were almost equal in the Aksu River subbasin.

3) In the Tarim River basin, the runoff generated by rainfall was the dominant component in spring, autumn, and winter, while glacier melt runoff was the dominant component in summer. Glaciers melted from April to September, which was later than the peak of snowmelt.

4) In the Tarim River Basin overall, changes in river runoff were mainly caused by increased temperatures, which contributed 56.49%, while increased precipitation contributed 43.51%. Runoff increases in the large glacial river basin were caused by temperature increases, while runoff increases in the small glacial river basin were mainly caused by precipitation increases.

Supplementary material is available in the online version of this article at http://dx.doi.org/10.1007/s11707-022-0995-0 and is accessible for authorized users.

Acknowledgment This study was supported by the National Natural Science Foundation of China (Grant Nos. 41671211 and 42261144002), the West Light Foundation of the Chinese Academy of Sciences (Nos. 2019-XBQNXZ-B-004 and 2019-XBYJRC-001), the Key Research Program by Jiangxi Meteorological Bureau (No. JX201810).

References

Ali A F, Xiao C D, Zhang X P, Adnan M, Iqbal M, Khan G (2018). Projection of future streamflow of the Hunza River Basin, Karakoram Range (Pakistan) using HBV hydrological model. J Mt Sci, 15(10): 2218–2235

Bolch T, Duethmann D, Wortmann M, Liu S Y, Disse M (2022). Declining glaciers endanger sustainable development of the oases along the Aksu-Tarim River (Central Asia). Int J Sustain Dev World Ecol, 29(3): 209–218

Bouraoui F, Grizzetti B, Granlund K, Rekolainen S, Bidoglio G (2004). Impact of climate change on the water cycle and nutrient losses in a finnish catchment. Clim Change, 66(1–2): 109–126

Chen H, Chen Y, Li W, Li Z (2019). Quantifying the contributions of snow/glacier meltwater to river runoff in the Tianshan Mountains, Central Asia. Global Planet Change, 174: 47–57

Chen H, Xu C Y, Guo S (2012). Comparison and evaluation of multiple GCMs, statistical downscaling and hydrological models in the study of climate change impacts on runoff. J Hydrol (Amst), 434–435: 36–45

Chen Y N, Li W H, Xu C C, Hao X M (2007). Effects of climate change on water resources in Tarim River Basin, Northwest China. J Environ Sci (China), 19(4): 488–493

Chen Y N, Xu C C, Hao X M, Li W H, ChenY P, Zhu C G, Ye Z X (2009). Fifty-year climate change and its effect on annual runoff in

the Tarim River Basin, China. Quat Int, 208(1): 53–61

Duethmann D, Bolch T, Farinotti D, Kriegel D, Vorogushyn S, Merz B, Pieczonka T, Jiang T, Su B, Güntner A (2015). Attribution of streamflow trends in snow and glacier melt-dominated catchments of the Tarim River, Central Asia. Water Resour Res, 51(6): 4727–4750

Etter S, Addor N, Huss M, Finger D (2017). Climate change impacts on future snow, ice and rain runoff in a Swiss mountain catchment using multi-dataset calibration. J Hydrol Reg Stud, 13: 222–239

Fan M, Xu J, Chen Y, Li W (2021). Modeling streamflow driven by climate change in data-scarce mountainous basins. Sci Total Environ, 790: 148256

Farinotti D, Longuevergne L, Moholdt G, Duethmann D, Mölg T, Bolch T, Vorogushyn S, Güntner A (2015). Substantial glacier mass loss in the Tien Shan over the past 50 years. Nat Geosci, 8(9): 716–722

Fonley M, Mantilla R, Curtu R (2019). Doing hydrology backwards—analytic solution connecting streamflow oscillations at the basin outlet to average evaporation on a hillslope. Hydrology, 6(4): 85

Frey H, Machguth H, Huss M, Huggel C, Bajracharya S, Bolch T, Kulkarni A, Linsbauer A, Salzmann N, Stoffel M (2014). Estimating the volume of glaciers in the Himalayan-Karakoram region using different methods. Cryosphere, 8(6): 2313–2333

Guo J, Huang G, Wang X, Wu Y, Li Y, Zheng R, Song L (2020). Evaluating the added values of regional climate modeling over China at different resolutions. Sci Total Environ, 718: 137350

Gupta H V, Kling H, Yilmaz K K, Martinez G F (2009). Decomposition of the mean squared error and NSE performance criteria: implications for improving hydrological modelling. J Hydrol (Amst), 377(1–2): 80–91

Haeberli W, Hoelzle M (1995). Application of inventory data for estimating characteristics of and regional climate-change effects on mountain glaciers: a pilot study with the European Alps. Ann Glaciol, 21: 206–212

Harris I, Jones P D, Osborn T J, Lister D H (2014). Updated high-resolution grids of monthly climatic observations — the CRU TS3.10 Dataset. Int J Climatol, 34(3): 623–642

He Z, Duethmann D, Tian F (2021). A meta-analysis based review of quantifying the contributions of runoff components to streamflow in glacierized basins. J Hydrol (Amst), 603: 126890

Huang S, Wortmann M, Duethmann D, Menz C, Shi F, Zhao C, Su B, Krysanova V (2018). Adaptation strategies of agriculture and water management to climate change in the Upper Tarim River basin, NW China. Agric Water Manage, 203: 207–224

Idrizovic D, Pocuca V, Vujadinovic Mandic M, Djurovic N, Matovic G, Gregoric E (2020). Impact of climate change on water resource availability in a mountainous catchment: a case study of the Toplica River catchment, Serbia. J Hydrol (Amst), 587: 124992

Immerzeel W W, Pellicciotti F, Bierkens M F P (2013). Rising river flows throughout the twenty-first century in two Himalayan glacierized watersheds. Nat Geosci, 6(9): 742–745

Ji H, Fang G, Yang J, Chen Y (2019). Multi-objective calibration of a distributed hydrological model in a highly glacierized watershed in Central Asia. Water, 11(3): 554

Kling H, Fuchs M, Paulin M (2012). Runoff conditions in the upper Danube basin under an ensemble of climate change scenarios. J Hydrol (Amst), 424–425: 264–277

Knoben W J M, Freer J E, Woods R A (2019). Technical note: inherent benchmark or not? Comparing Nash–Sutcliffe and Kling–Gupta efficiency scores. Hydrol Earth Syst Sci, 23(10): 4323–4331

Konz M, Seibert J (2010). On the value of glacier mass balances for hydrological model calibration. J Hydrol (Amst), 385(1–4): 238–246

Legates D R, McCabe G J Jr (1999). Evaluating the use of "goodness-of-fit" measures in hydrologic and hydroclimatic model validation. Water Resour Res, 35(1): 233–241

Li C, Fang H (2021). Assessment of climate change impacts on the streamflow for the Mun River in the Mekong Basin, Southeast Asia: using SWAT model. Catena, 201: 105199

Li H, Beldring S, Xu C Y, Huss M, Melvold K, Jain S K (2015). Integrating a glacier retreat model into a hydrological model — case studies of three glacierised catchments in Norway and Himalayan region. J Hydrol (Amst), 527: 656–667

Li Z, Shi X, Tang Q, Zhang Y, Gao H, Pan X, Déry S J, Zhou P (2020). Partitioning the contributions of glacier melt and precipitation to the 1971–2010 runoff increases in a headwater basin of the Tarim River. J Hydrol (Amst), 583: 124579

Linsbauer A, Paul F, Haeberli W (2012). Modeling glacier thickness distribution and bed topography over entire mountain ranges with GlabTop: application of a fast and robust approach. J Geophys Res Earth Surf, 117: F03007

Lutz A F, Immerzeel W W, Shrestha A B, Bierkens M F P (2014). Consistent increase in High Asia's runoff due to increasing glacier melt and precipitation. Nat Clim Chang, 4(7): 587–592

Lyu J, Shen B, Li H (2015). Dynamics of major hydro-climatic variables in the headwater catchment of the Tarim River Basin, Xinjiang, China. Quat Int, 380–381: 143–148

Moriasi D N, Arnold J G, Van Liew M W, Bingner R L, Harmel R D, Veith T L (2007). Model evaluation guidelines for systematic quantification of accuracy in watershed simulations. Trans ASABE, 50(3): 885–900

Nash J E, Sutcliffe J V (1970). River flow forecasting through conceptual models part I — a discussion of principles. J Hydrol (Amst), 10(3): 282–290

Nie Y, Pritchard H D, Liu Q, Hennig T, Wang W, Wang X, Liu S, Nepal S, Samyn D, Hewitt K, Chen X (2021). Glacial change and hydrological implications in the Himalaya and Karakoram. Nat Rev Earth Environ, 2(2): 91–106

Pfeffer W T, Arendt A A, Bliss A, Bolch T, Cogley J G, Gardner A S, Hagen J O, Hock R, Kaser G, Kienholz C, Miles E S, Moholdt G, Mölg N, Paul F, Radić V, Rastner P, Raup B H, Rich J, Sharp M J (2014). The Randolph Glacier Inventory: a globally complete inventory of glaciers. J Glaciol, 60(221): 537–552

Press W H, Teukolsky S A, Vetterling W T, Flannery B P (2002). Numerical Recipes in C++: The Art of Scientific Computing (2nd ed). London: Cambridge University Press

Pritchard H D (2019). Asia's shrinking glaciers protect large populations from drought stress. Nature, 569(7758): 649–654

Seibert J (2000). Multi-criteria calibration of a conceptual runoff model

using a genetic algorithm. Hydrol Earth Syst Sci, 4(2): 215–224

Seibert J, Vis M J P (2012). Teaching hydrological modeling with a user-friendly catchment-runoff-model software package. Hydrol Earth Syst Sci, 16(9): 3315–3325

Seibert J, Vis M J P, Kohn I, Weiler M, Stahl K (2018). Technical note: representing glacier geometry changes in a semi-distributed hydrological model. Hydrol Earth Syst Sci, 22(4): 2211–2224

Seiller G, Anctil F (2014). Climate change impacts on the hydrologic regime of a Canadian river: comparing uncertainties arising from climate natural variability and lumped hydrological model structures. Hydrol Earth Syst Sci, 18(6): 2033–2047

Shi Y, Shen Y, Li D, Zhang G, Ding Y, Hu R, Kang E (2003). Discussion on the present climate change from warm-dry to warm-wet in northwest China. Quat Sci, 23(2): 152–164 (in Chinese)

Su B, Jian D, Li X, Wang Y, Wang A, Wen S, Tao H, Hartmann H (2017). Projection of actual evapotranspiration using the COSMO-CLM regional climate model under global warming scenarios of 1.5°C and 2.0°C in the Tarim River basin, China. Atmos Res, 196: 119–128

Su B, Wang A, Wang G, Wang Y, Jiang T (2016). Spatiotemporal variations of soil moisture in the Tarim River basin, China. ITC J, 48: 122–130

Tao H, Gemmer M, Bai Y, Su B, Mao W (2011). Trends of streamflow in the Tarim River basin during the past 50 years: human impact or climate change? J Hydrol (Amst), 400(1–2): 1–9

Wang A, Wang Y, Su B, Kundzewicz Z W, Tao H, Wen S, Qin J, Gong Y, Jiang T (2020). Comparison of changing population exposure to droughts in river basins of the Tarim and the Indus. Earth's Future, 8(5): e2019EF001448

Wang C, Xu J, Chen Y, Bai L, Chen Z (2018). A hybrid model to assess the impact of climate variability on streamflow for an ungauged mountainous basin. Clim Dyn, 50(7–8): 2829–2844

Wang C, Xu J, Chen Y, Li W (2019a). An approach to simulate the climate-driven streamflow in the data-scarce mountain basins of Northwest China. J Earth Syst Sci, 128(4): 95

Wang X, Luo Y, Sun L, Shafeeque M (2021). Different climate factors contributing for runoff increases in the high glacierized tributaries of Tarim River Basin, China. J Hydrol Reg Stud, 36: 100845

Wang X, Luo Y, Sun L, Zhang Y (2015). Assessing the effects of precipitation and temperature changes on hydrological processes in a glacier-dominated catchment. Hydrol Processes, 29(23): 4830–4845

Wang X, Yang T, Xu C Y, Yong B, Shi P (2019b). Understanding the discharge regime of a glacierized alpine catchment in the Tianshan Mountains using an improved HBV-D hydrological model. Global Planet Change, 172: 211–222

Wu J, Gao X (2013). A gridded daily observation dataset over China region and comparison with the other dataset. Chin J Geophys, 56(04): 1102–1111 (in Chinese)

Wu J, Gao X, Giorgi F, Chen D (2017). Changes of effective temperature and cold/hot days in late decades over China based on a high resolution gridded observation dataset. Int J Climatol, 37(S1): 788–800

Wu Y, Fang H, Huang L, Ouyang W (2020). Changing runoff due to temperature and precipitation variations in the dammed Jinsha River. J Hydrol (Amst), 582: 124500

Xin J, Sun X, Liu L, Li H, Liu X, Li X, Cheng L, Xu Z (2021). Quantifying the contribution of climate and underlying surface changes to alpine runoff alterations associated with glacier melting. Hydrol Processes, 35(3): e14069

Xu J, Koldunov N, Remedio A R C, Sein D V, Zhi X, Jiang X, Xu M, Zhu X, Fraedrich K, Jacob D (2018). On the role of horizontal resolution over the Tibetan Plateau in the REMO regional climate model. Clim Dyn, 51(11–12): 4525–4542

Xu M, Han H, Kang S (2017). Modeling glacier mass balance and runoff in the Koxkar River Basin on the south slope of the Tianshan Mountains, China, from 1959 to 2009. Water, 9(2): 100

Xu Z, Liu Z, Fu G, Chen Y (2010). Trends of major hydroclimatic variables in the Tarim River basin during the past 50 years. J Arid Environ, 74(2): 256–267

Ye Z, Chen Y, Li W (2014a). Ecological water rights and water-resource exploitation in the three headwaters of the Tarim River. Quat Int, 336: 20–25

Ye Z, Chen Y, Zhang X (2014b). Dynamics of runoff, river sediments and climate change in the upper reaches of the Tarim River, China. Quat Int, 336: 13–19

Zhang X Y, Zuo Q T (2017). Analysis of series variational characteristics and causes of Tarim River Basin runoff under the changing environment. Appl Ecol Environ Res, 15(3): 823–836

Zhang Z, Hu H, Tian F, Yao X, Sivapalan M (2014). Groundwater dynamics under water-saving irrigation and implications for sustainable water management in an oasis: Tarim River basin of western China. Hydrol Earth Syst Sci, 18(10): 3951–3967

Zhao Q, Ye B, Ding Y, Zhang S, Yi S, Wang J, Shangguan D, Zhao C, Han H (2013). Coupling a glacier melt model to the Variable Infiltration Capacity (VIC) model for hydrological modeling in north-western China. Environ Earth Sci, 68(1): 87–101